Parallel dynamics of disordered Ising spin systems on finitely connected random graphs

J P L Hatchett[†], **B Wemmenhove**[¶], **I Pérez Castillo**[‡],
T Nikoletopoulos[†], **N S Skantzos**[§] **and A C C Coolen**[†]

† Department of Mathematics, King's College London,
  The Strand, London WC2R 2LS, United Kingdom
¶ Institute for Theoretical Physics, University of Amsterdam,
  Valckenierstraat 65, 1018 XE Amsterdam, The Netherlands
‡ Institute for Theoretical Physics, Katholieke Universiteit Leuven,
  Celestijnenlaan 200D, B-3001 Belgium
§ Departament de Física Fonamental, Facultat de Física, Universitat de Barcelona,
  08028 Barcelona, Spain

Abstract. We study the dynamics of bond-disordered Ising spin systems on random graphs with finite connectivity, using generating functional analysis. Rather than disorder-averaged correlation and response functions (as for fully connected systems), the dynamic order parameter is here a measure which represents the disorder averaged single-spin path probabilities, given external perturbation field paths. In the limit of completely asymmetric graphs our macroscopic laws close already in terms of the single-spin path probabilities at zero external field. For the general case of arbitrary graph symmetry we calculate the first few time steps of the dynamics exactly, and we work out (numerical and analytical) procedures for constructing approximate stationary solutions of our equations. Simulation results support our theoretical predictions.

1. Introduction

Recently there has been much interest in the study of randomly but finitely connected disordered spin models. In physics they have the appeal of appearing closer to genuinely finite dimensional systems than their fully connected mean field counterparts. Furthermore, finitely connected models are found to exhibit many interesting and complex new features which are worthy of analysis. Their equilibrium properties have been studied in the context of spin glasses [1, 2, 3, 4, 5, 6], error correcting codes [7, 8, 9], satisfiability problems [10, 11, 12, 13], neural networks [14, 15] and 'small world' models [16, 17]. Such analyses involve order parameter functions, which generalize the replica matrices of [18]. The finite connectivity replica symmetry breaking theory (RSB) is still

under development [5, 19, 20, 21, 6, 22]. It appears that virtually all studies thus far have concentrated on equilibrium properties or microscopic approximation schemes [23], with the exception of a spherical model [24].

In this paper we analyze the dynamics of finitely connected disordered Ising spin models using the generating functional method of [25], which has a strong record in disordered spin systems, particularly in applications to systems with non-symmetric bonds (e.g. [26, 27, 28, 29]). Here we apply this method to randomly and finitely connected Ising spin models with independently drawn random bonds and synchronous spin updates. The random connectivity graphs are generated such as to allow for a controlled degree of symmetry. In the thermodynamic limit one then finds a closed theory, describing an effective single spin problem with dynamic order parameters which represent the probabilities of single-spin paths, conditional on external field paths.

For fully asymmetric systems our equations simplify and close already for the single-spin path probabilities without external fields. Now one can solve various models completely, including phase diagrams. We work out the theory for finitely connected ferromagnets, and spin glass models with $\pm J$ or Gaussian random bonds. Application to neural networks (after adaptation of the theory, since here the bonds are no longer statistically independent) recovers and complements results of [30], which were originally found via counting arguments. As usual, the simplifications found for asymmetric dilution can be traced back to the absence of loops in the asymmetric random graph (see e.g. [30, 31]).

Away from asymmetric dilution, i.e. in the nontrivial regime, we calculate the single-spin path probabilities for the first few time steps exactly. We also approximate the stationary state solution numerically by truncating the single-spin paths. This approximation is controlled, in that it improves systematically upon increasing the number of time steps taken into account. However, as the dynamics slows down near phase transitions and for low temperatures, the accuracy of such numerics demands an increasingly heavy price in CPU since the dimension of the space of probabilities over paths grows exponentially with the length of paths. Finally we construct explicit approximations for the stationary solution of our equations for the case of symmetric dilution, in terms of an effective field distribution, which is shown to reduce to the RS equilibrium theory corresponding to sequential dynamics, at least in leading nontrivial order in the inverse average connectivity c^{-1}. Throughout this paper we present results of numerical simulations in support of our theoretical findings.

2. Model definitions

Our model consists of N Ising spins $\sigma_i \in \{-1, 1\}$ on a random graph. Their dynamics are given by a Markovian process which describes synchronous stochastic alignment of the spins to local fields of the form $h_i(\boldsymbol{\sigma}; t) = c^{-1} \sum_{j \neq i} c_{ij} J_{ij} \sigma_j + \theta_i(t)$, with $\boldsymbol{\sigma} = (\sigma_1, \ldots, \sigma_N) \in \{-1, 1\}^N$. Upon defining $p_t(\boldsymbol{\sigma})$ as the probability to find the system

at time t in microscopic state $\boldsymbol{\sigma}$, this process can be written as

$$p_{t+1}(\boldsymbol{\sigma}) = \sum_{\boldsymbol{\sigma}'} W_t[\boldsymbol{\sigma}; \boldsymbol{\sigma}'] p_t(\boldsymbol{\sigma}') \qquad W_t[\boldsymbol{\sigma}; \boldsymbol{\sigma}'] = \prod_i \frac{e^{\beta \sigma_i h_i(\boldsymbol{\sigma}';t)}}{2 \cosh[\beta h_i(\boldsymbol{\sigma}'; t)]} \qquad (1)$$

The parameter $\beta = T^{-1}$ measures the noise in the dynamics, which becomes fully random for $\beta = 0$ and fully deterministic for $\beta \to \infty$. The (symmetric) bonds $J_{ij} = J_{ji}$ are drawn independently from a probability distribution $\tilde{P}(J)$. The $\theta_i(t)$ define external (perturbation) fields. The $c_{ij} \in \{0, 1\}$ specify the microscopic realization of the graph, and are chosen randomly and independently according to

$$i < j: \quad P(c_{ij}) = \frac{c}{N} \delta_{c_{ij},1} + (1 - \frac{c}{N}) \delta_{c_{ij},0} \tag{2}$$

$$i > j: \quad P(c_{ij}) = \epsilon \delta_{c_{ij},c_{ji}} + (1 - \epsilon)[\frac{c}{N} \delta_{c_{ij},1} + (1 - \frac{c}{N}) \delta_{c_{ij},0}] \tag{3}$$

The average number of connections per spin c is assumed to remain finite in the limit $N \to \infty$. The parameter $\epsilon \in [0, 1]$ controls the symmetry of the graph. The microscopic graph and bond variables $\{c_{ij}, J_{ij}\}$ are regarded as quenched disorder. We write averages over the process (1) as $\langle \cdots \rangle$, averages over the disorder as $\overline{\cdots}$, and $\int dJ \ \tilde{P}(J) f(J)$ as $\langle f(J) \rangle_J$. Detailed balance holds only for $\epsilon = 1$, still we will find (in theory and simulations) that also for $\epsilon < 1$ a macroscopic stationary state is approached as $t \to \infty$.

3. Generating functional analysis

Following [25] we assume that for $N \to \infty$ the macroscopic behaviour of the system depends only on the statistical properties of the disorder (the system is self-averaging), and we concentrate on the calculation of the disorder averaged generating functional

$$\overline{Z[\boldsymbol{\psi}]} = \overline{\langle \exp[-i \sum_i \sum_{t \leq t_m} \psi_i(t) \sigma_i(t)] \rangle}$$

$$= \sum_{\boldsymbol{\sigma}(0)} \cdots \sum_{\boldsymbol{\sigma}(t_m)} \overline{P[\boldsymbol{\sigma}(0), \ldots, \boldsymbol{\sigma}(t_m)] \exp[-i \sum_i \sum_t \psi_i(t) \sigma_i(t)]} \tag{4}$$

We isolate the local fields in the usual manner via delta functions, which gives

$$\overline{Z[\boldsymbol{\psi}]} = \int \{d\mathbf{h} d\hat{\mathbf{h}}\} \sum_{\boldsymbol{\sigma}(0)} \cdots \sum_{\boldsymbol{\sigma}(t_m)} p(\boldsymbol{\sigma}(0)) e^{N\mathcal{F}[\{\boldsymbol{\sigma}\}, \{\hat{\mathbf{h}}\}]}$$

$$\times \prod_{it} e^{i\hat{h}_i(t)[h_i(t) - \theta_i(t)] - \psi_i(t)\sigma_i(t) + \beta \sigma_i(t+1)h_i(t) - \log 2 \cosh[\beta h_i(t)]} \tag{5}$$

$$\mathcal{F}[\{\boldsymbol{\sigma}\}, \{\hat{\mathbf{h}}\}] = N^{-1} \log \overline{[e^{-\frac{i}{c} \sum_{it} \hat{h}_i(t) \sum_j c_{ij} J_{ij} \sigma_j(t)}]} \tag{6}$$

with $\{d\mathbf{h} d\hat{\mathbf{h}}\} = \prod_{it}[dh_i(t) d\hat{h}_i(t)/2\pi]$. Upon performing the disorder average in (6) one finds, as always for finite connectivity models, expressions involving exponentials of exponentials. Site factorization in (5) can now be achieved, provided we choose initializations of the form $p_0(\boldsymbol{\sigma}(0)) = \prod_i p_0(\sigma_i(0))$, if we insert $1 = \sum_{\boldsymbol{\sigma}} \delta_{\boldsymbol{\sigma}, \boldsymbol{\sigma}_i} \int d\hat{\mathbf{h}} \ \delta(\hat{\mathbf{h}} - \hat{\mathbf{h}}_i)$ for all i and subsequently isolate

$$P(\boldsymbol{\sigma}, \hat{\mathbf{h}}; \{\sigma_i(t), \hat{h}_i(t)\}) = N^{-1} \sum_i \delta_{\boldsymbol{\sigma}, \boldsymbol{\sigma}_i} \delta(\hat{\mathbf{h}} - \hat{\mathbf{h}}_i) \tag{7}$$

Now vectors refer to paths: $\boldsymbol{\sigma}_i = (\sigma_i(0), \sigma_i(1), \sigma_i(2), \ldots)$, and similar for $\hat{\mathbf{h}}_i$. All this results in an expression for $\overline{Z[\boldsymbol{\psi}]}$ which can be evaluated by steepest descent:

$$\overline{Z[\ldots]} = \int \{dP d\hat{P}\} \, e^{N\Psi[\{P,\hat{P}\}]} \tag{8}$$

$$\Psi[\ldots] = i \int d\hat{\mathbf{h}} \sum_{\boldsymbol{\sigma}} \hat{P}(\boldsymbol{\sigma}, \hat{\mathbf{h}}) P(\boldsymbol{\sigma}, \hat{\mathbf{h}}) + \frac{c}{2} \int d\hat{\mathbf{h}} d\hat{\mathbf{h}}' \sum_{\boldsymbol{\sigma}, \boldsymbol{\sigma}'} P(\boldsymbol{\sigma}, \hat{\mathbf{h}}) P(\boldsymbol{\sigma}', \hat{\mathbf{h}}') A(\boldsymbol{\sigma}, \hat{\mathbf{h}}; \boldsymbol{\sigma}', \hat{\mathbf{h}}')$$

$$+ \log \sum_{\boldsymbol{\sigma}} p_0(\sigma(0)) \int \prod_t \left[\frac{dh(t) d\hat{h}(t)}{2\pi} \frac{e^{i\hat{h}(t)[h(t) - \theta(t)] + \beta\sigma(t+1)h(t)}}{2\cosh[\beta h(t)]} \right] e^{-i\hat{P}(\boldsymbol{\sigma}, \hat{\mathbf{h}})} \tag{9}$$

with

$$A(\boldsymbol{\sigma}, \hat{\mathbf{h}}; \boldsymbol{\sigma}', \hat{\mathbf{h}}') = \left\langle \epsilon e^{-i\frac{J}{c}(\boldsymbol{\sigma} \cdot \hat{\mathbf{h}}' + \boldsymbol{\sigma}' \cdot \hat{\mathbf{h}})} + (1-\epsilon) e^{-i\frac{J}{c}\boldsymbol{\sigma} \cdot \hat{\mathbf{h}}'} + (1-\epsilon) e^{-i\frac{J}{c}\boldsymbol{\sigma}' \cdot \hat{\mathbf{h}}} - 2 + \epsilon \right\rangle_J \tag{10}$$

(in which we have neglected contributions which will vanish for $N \to \infty$, and eliminated the now redundant generating fields $\boldsymbol{\psi}$). Functional variation of $\Psi[\ldots]$ with respect to $P(\boldsymbol{\sigma}, \hat{\mathbf{h}})$ and $\hat{P}(\boldsymbol{\sigma}, \hat{\mathbf{h}})$ gives the following saddle-point equations, respectively:

$$\hat{P}(\boldsymbol{\sigma}, \hat{\mathbf{h}}) = ic \sum_{\boldsymbol{\sigma}'} \int d\hat{\mathbf{h}}' A(\boldsymbol{\sigma}, \hat{\mathbf{h}}; \boldsymbol{\sigma}', \hat{\mathbf{h}}') P(\boldsymbol{\sigma}', \hat{\mathbf{h}}') \tag{11}$$

$$P(\boldsymbol{\sigma}', \hat{\mathbf{h}}') = \langle \delta_{\boldsymbol{\sigma}', \boldsymbol{\sigma}} \delta[\hat{\mathbf{h}}' - \hat{\mathbf{h}}] \rangle_{\boldsymbol{\theta}} \tag{12}$$

with a measure $\langle \ldots \rangle_{\boldsymbol{\theta}}$ which can be interpreted in terms of an effective single spin:

$$\langle f(\boldsymbol{\sigma}, \hat{\mathbf{h}}) \rangle_{\boldsymbol{\theta}} = \frac{\sum_{\boldsymbol{\sigma}} \int d\hat{\mathbf{h}} \, f(\boldsymbol{\sigma}, \hat{\mathbf{h}}) M(\boldsymbol{\sigma}, \hat{\mathbf{h}}|\boldsymbol{\theta})}{\sum_{\boldsymbol{\sigma}} \int d\hat{\mathbf{h}} \, M(\boldsymbol{\sigma}, \hat{\mathbf{h}}|\boldsymbol{\theta})} \tag{13}$$

$$M(\boldsymbol{\sigma}, \hat{\mathbf{h}}|\boldsymbol{\theta}) = p_0(\sigma(0)) e^{-i\hat{P}(\boldsymbol{\sigma}, \hat{\mathbf{h}})} \int \prod_{t \geq 0} \left[\frac{dh(t)}{2\pi} \frac{e^{i\hat{h}(t)[h(t) - \theta(t)] + \beta\sigma(t+1)h(t)}}{2\cosh[\beta h(t)]} \right] \tag{14}$$

To infer the physical meaning of (12) we write the delta function over $\hat{\mathbf{h}}$ in integral form and expand the exponential containing the conjugate fields. We can identify powers of the conjugate fields with derivatives with respect to our external field $\theta(t)$, resulting in

$$P(\boldsymbol{\sigma}, \hat{\mathbf{h}}) = \int \frac{d\boldsymbol{\theta}'}{(2\pi)^{t_m}} e^{i\boldsymbol{\theta}' \cdot \hat{\mathbf{h}} + \boldsymbol{\theta}' \cdot \nabla_{\boldsymbol{\theta}}} \langle \delta_{\boldsymbol{\sigma}, \boldsymbol{\sigma}'} \rangle_{\boldsymbol{\theta}} \tag{15}$$

Using $e^{\boldsymbol{\theta}' \cdot \nabla_x} f(\mathbf{x}) = f(\mathbf{x} + \boldsymbol{\theta}')$ and performing an inverse Fourier transform gives

$$P(\boldsymbol{\sigma}|\boldsymbol{\theta}') \equiv \int d\hat{\mathbf{h}} \, e^{-i\boldsymbol{\theta}' \cdot \hat{\mathbf{h}}} P(\boldsymbol{\sigma}, \hat{\mathbf{h}}) = \langle \delta_{\boldsymbol{\sigma}, \boldsymbol{\sigma}'} \rangle_{\boldsymbol{\theta} + \boldsymbol{\theta}'} \tag{16}$$

Thus $P(\boldsymbol{\sigma}|\boldsymbol{\theta}')$ is the disorder-averaged probability of finding a single-spin trajectory $\boldsymbol{\sigma}$, given that the actual local field path $\boldsymbol{\theta}$ is complemented by an amount $\boldsymbol{\theta}'$, similarly to what was found in the spherical case [24].

Finally we expand (14) in powers of $\hat{P}(\boldsymbol{\sigma}, \hat{\mathbf{h}})$, substitute (11), and integrate out all conjugate fields. This results in the following compact form of our equations:

$$P(\boldsymbol{\sigma}|\boldsymbol{\theta}') = \sum_{k \geq 0} \frac{e^{-c} c^k}{k!} \prod_{0 < \ell \leq k} \left\{ \int dJ_\ell \tilde{P}(J_\ell) \sum_{\boldsymbol{\sigma}_\ell} \left[\epsilon P(\boldsymbol{\sigma}_\ell | \frac{J_\ell \boldsymbol{\sigma}}{c}) + (1 - \epsilon) P(\boldsymbol{\sigma}_\ell | \mathbf{0}) \right] \right\}$$

$$\times p(\sigma(0)) \prod_{t \geq 0} \frac{e^{\beta\sigma(t+1)[\theta(t) + \theta'(t) + \sum_{0 < \ell \leq k} \frac{J_\ell \sigma_\ell(t)}{c}]}}{2\cosh(\beta[\theta(t) + \theta'(t) + \sum_{0 < \ell \leq k} \frac{J_\ell \sigma_\ell(t)}{c}])} \tag{17}$$

This equation has a clear interpretation. To calculate the probability of seeing a single-site path $\boldsymbol{\sigma}$, first a Poissonian random number k is drawn (the number of bonds attached to this site). Next for all k attached sites, the associated spin paths are sampled according to their respective distributions, from which the path probability at the central site then follows (given the external fields and states of the connected spins, and taking into account the effective retarded self-interaction induced by connection symmetry).

4. Fully asymmetric connectivity

4.1. The reduced theory

In the fully asymmetric case $\epsilon = 0$ our equations (17) simplify considerably, and close already in terms of $P(\boldsymbol{\sigma}|\mathbf{0})$. The latter we will now simply denote as $P(\boldsymbol{\sigma})$, so

$$P(\boldsymbol{\sigma}) = p(\sigma(0)) \sum_{k \geq 0} \frac{e^{-c}c^k}{k!} \prod_{0 < \ell \leq k} \left\{ \int dJ_\ell \tilde{P}(J_\ell) \sum_{\boldsymbol{\sigma}_\ell} P(\boldsymbol{\sigma}_\ell) \right\}$$
$$\times \prod_{t \geq 0} \left\{ \frac{e^{\beta \sigma(t+1)[\theta(t) + \sum_{0 < \ell \leq k} \frac{J_\ell \sigma_\ell(t)}{c}]}}{2 \cosh(\beta[\theta(t) + \sum_{0 < \ell \leq k} \frac{J_\ell \sigma_\ell(t)}{c}])} \right\} \quad (18)$$

We next sum both sides of (18) over all spin states in $\boldsymbol{\sigma}$ except for one, say $\sigma(t+1)$. This leaves an equation with only single-time spin probabilities of the form $P(\sigma(t))$, which we subsequently write in their more conventional notation $P_t(\sigma)$‡:

$$P_{t+1}(\sigma) = \sum_{k \geq 0} \frac{e^{-c}c^k}{k!} \prod_{0 < \ell \leq k} \left\{ \int dJ_\ell \tilde{P}(J_\ell) \sum_{\sigma_\ell} P_t(\sigma_\ell) \right\} \frac{e^{\beta \sigma[\theta(t) + \sum_{0 < \ell \leq k} \frac{J_\ell \sigma_\ell}{c}]}}{2 \cosh(\beta[\theta(t) + \sum_{0 < \ell \leq k} \frac{J_\ell \sigma_\ell}{c}])} \quad (19)$$

As with infinite connectivity, the single time distribution $P_t(\sigma)$ obeys a Markovian equation, although it is not a chain. This is a consequence of the virtual absence of loops in the graph for asymmetric bonds (so there is no effective retarded self-interaction). Using the identity $P_t(\sigma) = \frac{1}{2}[1 + \sigma m(t)]$, where $m(t) = \langle \sigma(t) \rangle$, we can alternatively write (19) fully as an iteration for the effective single spin magnetization:

$$m(t+1) = \sum_{k \geq 0} \frac{e^{-c}c^k}{k!} 2^{-k} \prod_{0 < \ell \leq k} \left\{ \sum_{\sigma_\ell} [1 + \sigma_\ell m(t)] \right\} \langle \tanh(\beta[\theta(t) + \sum_{0 < \ell \leq k} \frac{J_\ell}{c} \sigma_\ell]) \rangle_{J_1 \ldots J_k} \quad (20)$$

The calculation of the co-variances $C(t, t') = \langle \sigma(t)\sigma(t') \rangle$ from (18) requires knowledge of the joint distribution $P(\sigma(t-1), \sigma(t'-1))$. Here we may use, for $t > t'$,

$$P(\sigma(t), \sigma(t')) = \frac{1}{4} [1 + m(t)\sigma(t) + m(t')\sigma(t') + C(t, t')\sigma(t)\sigma(t')]$$

leading to a closed expression involving only magnetizations and co-variances:

$$C(t, t') = \sum_{k \geq 0} \frac{e^{-c}c^k}{k!} 4^{-k} \prod_{0 < \ell \leq k} \left\{ \sum_{\sigma_\ell \sigma'_\ell} [1 + \sigma_\ell m(t-1) + \sigma'_\ell m(t'-1) + \sigma_\ell \sigma'_\ell C(t-1, t'-1)] \right\}$$
$$\times \langle \tanh(\beta[\theta(t-1) + \sum_{0 < \ell \leq k} \frac{J_\ell}{c} \sigma_\ell]) \tanh(\beta[\theta(t'-1) + \sum_{0 < \ell \leq k} \frac{J_\ell}{c} \sigma'_\ell]) \rangle_{J_1 \ldots J_k} \quad (21)$$

‡ Note that the $k = 0$ term simply equals $e^{-c}e^{\beta \sigma \theta(t)}/2 \cosh[\beta \theta(t)]$.

As a simple test of our results, we may work out the limit $c \to \infty$. We isolate in the right-hand sides of (20,21) the internal fields $v_k(t) = \sum_{0 < \ell \le k} \frac{J_\ell}{c} \sigma'_\ell$ (which exist only for $k > 0$), and calculate their lowest order moments, giving

$$\langle v_k(t) \rangle = \frac{k}{c} \langle J \rangle_J m(t) \qquad \langle v_k^2(t) \rangle = \langle v_k(t) \rangle^2 + \frac{k}{c^2} [\langle J^2 \rangle_J - \langle J \rangle_J^2 m^2(t)]$$

Averaging subsequently over the Poisson distributed k gives

$$\sum_{k \ge 0} \frac{e^{-c} c^k}{k!} \langle v_k(t) \rangle = \langle J \rangle_J m(t) \tag{22}$$

$$\sum_{k \ge 0} \frac{e^{-c} c^k}{k!} \langle v_k^2(t) \rangle = \langle J \rangle_J^2 m^2(t) + \mathcal{O}(c^{-1}) \qquad (c \to \infty) \tag{23}$$

Hence for $c \to \infty$ we may put $v(t) \to \langle J \rangle_J m(t)$ in (20,21), and find

$$m(t+1) = \tanh(\beta[\theta(t) + \langle J \rangle_J m(t)]) \qquad C(t,t') = m(t)m(t') \tag{24}$$

(recovering the equations as derived earlier in e.g. [30, 31], with a continuous P→F transition at $T_c = \langle J \rangle_J$). For finite c the scaling with c of coupling constants has no structural effects on the theory; when taking $c \to \infty$ this is obviously no longer true. For instance, for $\langle J \rangle_J = 0$ it is appropriate to re-scale $J_\ell \to \sqrt{c} J_\ell$, which would lead to the $v_k(t)$ becoming temporally correlated zero-average Gaussian variables for $c \to \infty$.

4.2. Random bond spin models with asymmetric finite connectivity

Let us now work out our equations and the physics they describe for asymmetric finitely connected spin-glasses with binary bonds, i.e. $\tilde{P}(J') = \frac{1}{2}(1+\eta)\delta[J'-J] + \frac{1}{2}(1-\eta)\delta[J'+J]$ (with $\eta \in [-1, 1]$). Here we find (20) reducing to

$$m(t+1) = \sum_{k \ge 0} \frac{e^{-c} c^k}{k!} \sum_{r=0}^{k} \binom{k}{r} \left(\frac{1 + \eta m(t)}{2} \right)^r \left(\frac{1 - \eta m(t)}{2} \right)^{k-r} \tanh(\beta[\theta(t) + \frac{J}{c}(2r - k)]) \tag{25}$$

Thus, in the absence of external fields, the stationary state magnetizations (if a stationary state exists) follow as the fixed-points of the non-linear map $F(m)$:

$$F(m) = \sum_{k \ge 0} \frac{e^{-c} c^k}{k!} 2^{-k} \sum_{r=0}^{k} \binom{k}{r} (1 + \eta m)^r (1 - \eta m)^{k-r} \tanh[\frac{\beta J}{c}(2r - k)] \tag{26}$$

Expansion of $F(m)$ for small m gives

$$F(m) = \eta m \sum_{k \ge 0} \frac{e^{-c} c^k}{k!} 2^{-k} \sum_{r=0}^{k} \binom{k}{r} |2r - k| \tanh[\frac{\beta J}{c}|2r - k|]$$

$$- \frac{1}{3} (\eta m)^3 \sum_{k \ge 2} \frac{e^{-c} c^k}{k!} 2^{-k} \sum_{r=2}^{k} \binom{k}{r} r(r-1)(3k + 2 - 4r) \tanh[\frac{\beta J}{c}(2r - k)] + \mathcal{O}(m^5) \tag{27}$$

Numerical evaluation of the cubic term shows it to be strictly non-positive, hence one only has continuous P→F transitions, occurring at the following critical value for η:

$$\text{P} \to \text{F}: \qquad \eta_c^{-1} = \sum_{k \ge 0} \frac{e^{-c} c^k}{k!} 2^{-k} \sum_{r=0}^{k} \binom{k}{r} |2r - k| \tanh[\frac{\beta J}{c}|2r - k|] \tag{28}$$
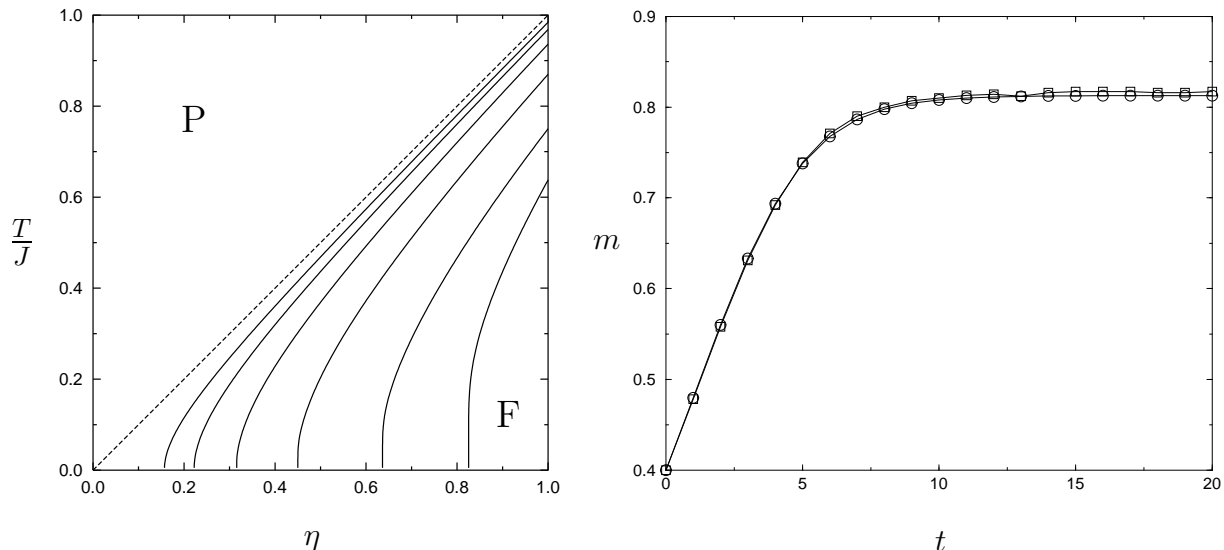
Figure 1. Left: phase diagram in the $(\eta, T/J)$ plane of the $\pm J$ random bond model on a Poissonian graph with asymmetric connectivity. Solid lines: P→F transition lines for $c = 2, 4, 8, 16, 32, 64$ (right to left). Dashed: the continuous transition at $T = \eta J$ corresponding to $c = \infty$. Right: comparison between theory and numerical simulations with respect to the evolution of the magnetization m, for $c = 5$, $\eta = 1$, and $T/J = 0.5$. Circles: solution of (25). Squares: simulation results for $N = 16,000$ spins (averaged over 10 runs). Time is discrete, so the line segments are only guides to the eye.

Similarly we can inspect the possible existence of a spin-glass type state, upon putting $m(t) \to 0$, removing external fields, and evaluating the bond averages in (21). The resulting equation is for time-translation invariant states found to be independent of the time arguments, and nontrivial solutions are fixed-points of a non-linear map $G(q)$ (without any dependence on η):

$$G(q) = \sum_{k \geq 0} \frac{e^{-c}c^k}{k!} \prod_{0 < \ell \leq k} \left\{ \frac{1}{4} \sum_{\sigma_\ell \sigma'_\ell} [1 + \sigma_\ell \sigma'_\ell q] \right\} \tanh[\frac{\beta J}{c} \sum_{0 < \ell \leq k} \sigma_\ell] \ \tanh[\frac{\beta J}{c} \sum_{0 < \ell \leq k} \sigma'_\ell] \quad (29)$$

Numerical inspection immediately shows that this equation has no non-trivial solutions; in Appendix A we give an analytical proof. We thus retain for asymmetric connectivity and $\pm J$ random bonds only two phases, a paramagnetic and a ferromagnetic one, separated by (28). The resulting phase diagrams are shown in figure 1, for different values of the connectivity c. In this figure we also show a comparison between the evolution of m as predicted by equation (25) and the evolution as measured in numerical simulations (here with for $c = 5$, $\eta = 1$, and $T/J = 0.5$). The agreement is excellent.

In a similar fashion we can work out the consequences of our equations (20,21) for asymmetric models with Gaussian random bonds, distributed according to $\tilde{P}(J') = (2\pi J^2)^{-\frac{1}{2}} e^{-\frac{1}{2}(J' - J_0)^2/J^2}$. We may now use the fact that the sum $\sum_{0 < \ell \leq k} (J_\ell/c)\sigma_\ell$ has become a Gaussian variable, with mean $(J_0/c) \sum_{0 < \ell \leq k} \sigma_\ell$ and variance kJ^2/c^2. In
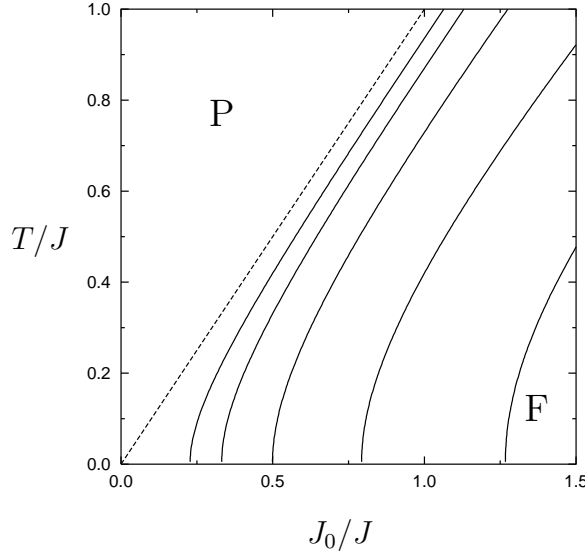
Figure 2. Phase diagram in the $(J_0/J, T/J)$ plane of the Gaussian random bond model on a Poissonian graph with finite asymmetric connectivity. Solid lines: P→F transition lines for $c = 2, 4, 8, 16, 32$ (from right to left). Dashed: the continuous transition at $T = J_0$ corresponding to $c = \infty$.

particular, in the absence of external fields the nonlinear map of which the fixed-point(s) give the spontaneous magnetization becomes

$$F(m) = \sum_{k \geq 0} \frac{e^{-c} c^k}{k!} 2^{-k} \sum_{r=0}^{k} \binom{k}{r} (1+m)^r (1-m)^{k-r} \int Dz \ \tanh[\frac{\beta J}{c}(\frac{J_0}{J}(2r-k) + z\sqrt{k})]$$

(30)

For small m one has

$$F(m) = m \sum_{k \geq 0} \frac{e^{-c} c^k}{k!} 2^{-k} \sum_{r=0}^{k} \binom{k}{r} |2r-k| \int Dz \ \tanh[\frac{\beta J}{c}(\frac{J_0}{J}|2r-k| + z\sqrt{k})]$$

$$- \frac{1}{3}(\eta m)^3 \sum_{k \geq 2} \frac{e^{-c} c^k}{k!} 2^{-k} \sum_{r=2}^{k} \binom{k}{r} r(r-1)(3k+2-4r)$$

$$\times \int Dz \ \tanh[\frac{\beta J}{c}(\frac{J_0}{J}(2r-k) + z\sqrt{k})] + \mathcal{O}(m^5)$$

(31)

with the abbreviation $Dz = (2\pi)^{-\frac{1}{2}} e^{-\frac{1}{2} z^2}$. Again the cubic term is found to be non-positive, which implies the prediction of a continuous P→F transition at

$$\text{P} \rightarrow \text{F}: \qquad 1 = \sum_{k \geq 0} \frac{e^{-c} c^k}{k!} 2^{-k} \sum_{r=0}^{k} \binom{k}{r} |2r-k| \int Dz \ \tanh[\frac{\beta J}{c}(\frac{J_0}{J}|2r-k| + z\sqrt{k})]$$

(32)

To identify possible P→SG transitions we again inspect (21) for $m = 0$ and without external fields. The time translation invariant solution represents the spin-glass order
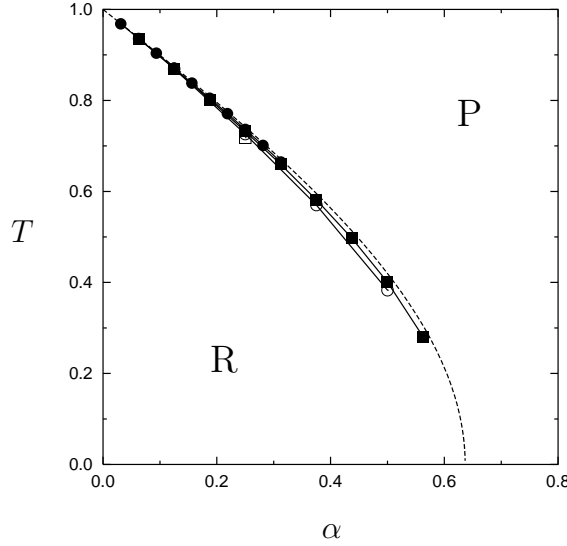
Figure 3. Phase diagram of attractor neural networks with Hebbian bonds (storing $p = \alpha c$ random patterns) and asymmetric finite connectivity, in the (α, T) plane. Both p and c are finite, so only the markers represent physical values; the line segments connecting markers are guides to the eye. The possible phases are P (paramagnetic) and R (pattern retrieval). The values of c shown are: $c = 4$ (open squares), $c = 8$ (open circles), $c = 16$ (full squares), and $c = 32$ (full circles). The dashed line is the transition corresponding to $c = \infty$ (at $T = 1 - \int Dz \ \tanh^2(\beta z \sqrt{\alpha})$, see e.g. [30]).

parameter q, and corresponds to the fixed-point of

$$G(q) = \sum_{k \geq 0} \frac{e^{-c}c^k}{k!} \prod_{0 < \ell \leq k} \left\{ \frac{1}{4} \sum_{\sigma_\ell \sigma'_\ell} [1 + \sigma_\ell \sigma'_\ell q] \right\} \int Dz_1 Dz_2 \ \tanh[\frac{\beta J}{c}(\frac{J_0}{J} \sum_{0 < \ell \leq k} \sigma'_\ell + \sqrt{k} z_2)]$$

$$\times \tanh[\frac{\beta J}{c}(\frac{J_0}{J} \sum_{0 < \ell \leq k} \sigma_\ell + z_1 \sqrt{k - \sum_{\ell \leq k} \sigma_\ell \sigma'_\ell} + \frac{z_2}{\sqrt{k}} \sum_{\ell \leq k} \sigma_\ell \sigma'_\ell)] \tag{33}$$

Again there are no nontrivial fixed-points of $G(q)$, and there is hence no P→SG transition (see Appendix A). The bottom line is that we again retain only two phases, a paramagnetic and a ferromagnetic one, separated now by (32). The resulting phase diagrams are shown in figure 2, for different values of the connectivity c.

4.3. Recurrent neural networks with asymmetric finite connectivity

Our third example of an Ising spin model on a random graph with finite asymmetric connectivity is a recurrent Hopfield type neural network. Such systems have already been studied earlier [30] (for the version with symmetric finite connectivity see [14]). Our objectives here are to see how earlier equations can be recovered from the present generating functional formalism, and to add new results (e.g. phase diagrams).

As before our model will be of the general form (1), but now those bonds present will have the values $J_{ij} = \sum_{\mu=1}^p \xi_i^\mu \xi_j^\mu$, with each of the p vectors $(\xi_1^\mu, \ldots, \xi_N^\mu) \in \{-1, 1\}^N$

denoting a (random) pattern stored. Here the different bonds are, although still random, no longer statistically independent, so that our equations are to be slightly modified. Instead of one path distribution $P(\boldsymbol{\sigma}) = \lim_{N\to\infty} N^{-1} \sum_i \delta_{\boldsymbol{\sigma},\boldsymbol{\sigma}_i}$, where $\boldsymbol{\sigma}_i = (\sigma_i(0), \sigma_i(1), \sigma_i(2), \ldots)$, we will now need 2^p different path distributions, one for each so-called sublattice $I_{\boldsymbol{\xi}} = \{i | \boldsymbol{\xi}_i = \boldsymbol{\xi}\}$, where $\boldsymbol{\xi}_i = \{\xi_i^1, \ldots \xi_i^p\}$. They are defined as $P_{\boldsymbol{\xi}}(\boldsymbol{\sigma}) = \lim_{N\to\infty} |I_{\boldsymbol{\xi}}|^{-1} \sum_{i\in I_{\boldsymbol{\xi}}} \delta_{\boldsymbol{\sigma},\boldsymbol{\sigma}_i}$. Equation (19) is now found to be replaced by

$$
\begin{aligned}
P_{\boldsymbol{\xi}}(\sigma(t+1)) = \sum_{k\geq 0} \frac{e^{-c}c^k}{k!} \Bigg\langle \ldots \Bigg\langle \prod_{0<\ell\leq k} \Bigg\{ \sum_{\sigma_\ell(t)} P_{\boldsymbol{\xi}_\ell}(\sigma_\ell(t)) \Bigg\} \\
\times \frac{e^{\beta\sigma(t+1)[\theta(t) + \sum_{0<\ell\leq k} \frac{\boldsymbol{\xi}\cdot\boldsymbol{\xi}_\ell}{c}\sigma_\ell(t))]}}{2\cosh(\beta[\theta(t) + \sum_{0<\ell\leq k}\frac{\boldsymbol{\xi}\cdot\boldsymbol{\xi}_\ell}{c}\sigma_\ell(t)])} \Bigg\rangle_{\boldsymbol{\xi}_1} \ldots \Bigg\rangle_{\boldsymbol{\xi}_k}
\end{aligned}
\tag{34}
$$

where $\langle f(\boldsymbol{\xi})\rangle_{\boldsymbol{\xi}} = 2^{-p}\sum_{\boldsymbol{\xi}\in\{-1,1\}^p} f(\boldsymbol{\xi})$. We define the sub-lattice magnetizations $m_{\boldsymbol{\xi}}(t) = \sum_{\sigma(t)} \sigma(t) P_{\boldsymbol{\xi}}(\sigma(t))$, and use the general identity $P_{\boldsymbol{\xi}}(\sigma(t)) = \frac{1}{2}[1 + \sigma(t)m_{\boldsymbol{\xi}}(t)]$ to convert (34) into the following counterpart of our previous non-linear iterative map (20):

$$
\begin{aligned}
m_{\boldsymbol{\xi}}(t+1) = \sum_{k\geq 0} \frac{e^{-c}c^k}{k!} 2^{-k} \Bigg\langle \ldots \Bigg\langle \prod_{0<\ell\leq k} \Bigg\{ \sum_{\sigma_\ell}[1 + \sigma_\ell m_{\boldsymbol{\xi}_\ell}(t)] \Bigg\} \\
\times \tanh(\beta[\theta(t) + \frac{1}{c}\sum_{0<\ell\leq k}\boldsymbol{\xi}\cdot\boldsymbol{\xi}_\ell\sigma_\ell]) \Bigg\rangle_{\boldsymbol{\xi}_1} \ldots \Bigg\rangle_{\boldsymbol{\xi}_k}
\end{aligned}
\tag{35}
$$

To determine the location of continuous phase transitions away from the paramagnetic stationary state solution $m_{\boldsymbol{\xi}} = 0$ for all $\boldsymbol{\xi}$, we expand the right-hand side of (35) for small $\{m_{\boldsymbol{\xi}}\}$ and absent external fields. Continuous bifurcations are then marked by the existence of non-trivial solutions for an eigenvalue problem, which upon carrying out suitable gauge transformations on the pattern variables, takes the shape

$$
m_{\boldsymbol{\xi}} = \sum_{k\geq 1} \frac{e^{-c}c^k}{k!} k \Bigg\langle \ldots \Bigg\langle m_{\boldsymbol{\xi}_1} \tanh(\frac{\beta}{c}[\boldsymbol{\xi}\cdot\boldsymbol{\xi}_1 + \sum_{1<\ell\leq k}(\sum_\mu \xi_\ell^\mu)]) \Bigg\rangle_{\boldsymbol{\xi}_1} \ldots \Bigg\rangle_{\boldsymbol{\xi}_k}
\tag{36}
$$

This eigenvalue equation is of the structural form $\sum_{\boldsymbol{\xi}'} U(\boldsymbol{\xi}\cdot\boldsymbol{\xi}')m_{\boldsymbol{\xi}'} = \lambda m_{\boldsymbol{\xi}}$, solved (in a different context) in [32]. Here we require eigenvalue 1, and we have

$$
\begin{aligned}
U(x) &= 2^{-p}c \sum_{k\geq 0} \frac{e^{-c}c^k}{k!} \Bigg\langle \ldots \Bigg\langle \tanh(\frac{\beta}{c}[x + \sum_{0<\ell\leq k}(\sum_\mu \xi_\ell^\mu)]) \Bigg\rangle_{\boldsymbol{\xi}_1} \ldots \Bigg\rangle_{\boldsymbol{\xi}_k} \\
&= 2^{-p}c \sum_{k\geq 0} \frac{e^{-c}c^k}{k!} 2^{-kp} \sum_{r=0}^{kp} \binom{kp}{r} \tanh(\frac{\beta}{c}[x + 2r - kp])
\end{aligned}
\tag{37}
$$

For each of the 2^p index subsets $S \subseteq \{1, 2, \ldots, p\}$ one obtains an eigenvalue [32]

$$
\begin{aligned}
\lambda_S &= \sum_{\boldsymbol{\xi}} U(\sum_{\nu=1}^p \xi^\nu) \prod_{\mu\in S} \xi^\mu \\
&= c \sum_{k\geq 0} \frac{e^{-c}c^k}{k!} 2^{-kp} \sum_{r=0}^{kp} \binom{kp}{r} \langle \Bigg\{ \prod_{\mu\in S} \xi^\mu \Bigg\} \tanh(\frac{\beta}{c}[\sum_{\nu=1}^p \xi^\nu + 2r - kp])\rangle_{\boldsymbol{\xi}}
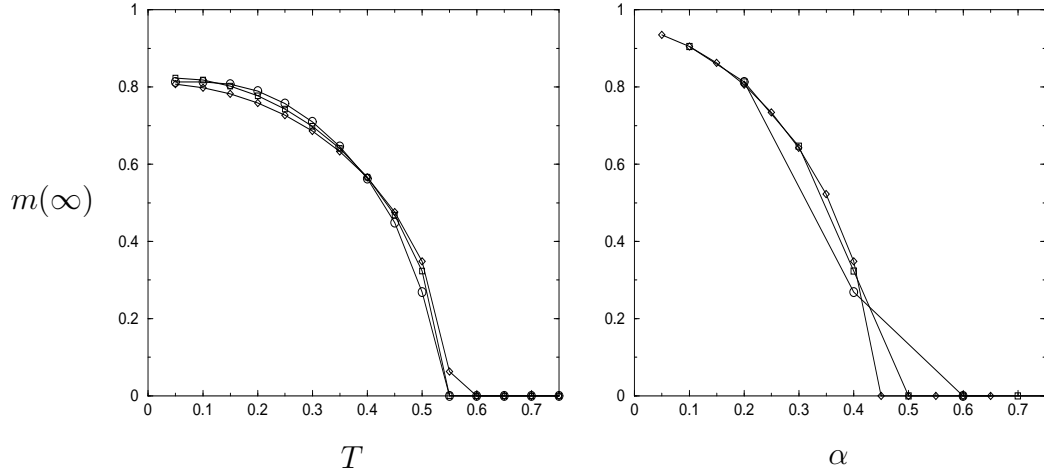\end{aligned}
$$

Figure 4. Examples of the stationary overlaps $m(\infty)$, i.e. fixed-points of the iterative map (39). Left: $m(\infty)$ as function of T, for $\alpha = 0.4$ and $c = 5$ (circles), $c = 10$ (squares) and $c = 20$ (diamonds). Here the transitions are predicted to occur at $T \simeq 0.52$, $T \simeq 0.54$ and $T \simeq 0.55$, respectively. Right: $m(\infty)$ as function of α, for $T = 0.5$ and $c = 5$ (circles), $c = 10$ (squares) and $c = 20$ (diamonds). Here the transitions are predicted to occur in the intervals $\alpha \in [0.4, 0.6]$, $\alpha \in [0.4, 0.5]$ and $\alpha \in [0.40, 0.45]$, respectively (α can only take values which are multiples of c^{-1}).

Since $\lim_{\beta \to 0} \lambda_S = 0$ for all index sets S, the phase transition corresponds to the highest temperature where the largest eigenvalue equals unity. The largest λ_S is found for index sets of size one; since the eigenvalue λ_S depends only on the size of the set S we may take $S = \{1\}$ and find the following equation for the transition line:

$$1 = c \sum_{k \geq 0} \frac{e^{-c} c^k}{k!} 2^{1-(k+1)p} \sum_{r=0}^{(k+1)p-1} \binom{(k+1)p-1}{r} \tanh(\frac{\beta}{c}[2 + 2r - (k+1)p]) \qquad (38)$$

This is shown in figure 3 in the (α, T) plane, where $\alpha = p/c$. Since both p and c are integers, the transition is for any given value of c marked by a discrete collection of points, which will only become a line for $c \to \infty$. We will confirm below that the bifurcating state is a recall state, so the two possible phases are P and R.

We may also make a so-called condensed ansatz, implying that we restrict ourselves to states having a macroscopic overlap with one pattern only. Since all patterns are equivalent, we may put $m_{\boldsymbol{\xi}}(t) = \xi^1 m(t)$ (see e.g. [14]). This gives self-consistent solutions of (35), with for $\theta(t) = 0$ the recall overlap m evolving according to

$$m(t+1) = \sum_{k \geq 0} \frac{e^{-c} c^k}{k!} \left\langle \ldots \left\langle \prod_{0 < \ell \leq k} \{1 + \xi_\ell^1 m(t)\} \tanh(\frac{\beta}{c} \sum_{0 < \ell \leq k} \sum_{\mu=1}^{p} \xi_\ell^\mu) \right\rangle_{\boldsymbol{\xi}_1} \ldots \right\rangle_{\boldsymbol{\xi}_k}$$

$$= \sum_{k \geq 0} \frac{e^{-c} c^k}{k!} 2^{-pk} \sum_{r=0}^{k(p-1)} \sum_{s=0}^{k} \binom{k(p-1)}{r} \binom{k}{s}$$

$$\times [1 + m(t)]^s [1 - m(t)]^{k-s} \tanh(\frac{\beta}{c}[2s + 2r - kp]) \qquad (39)$$
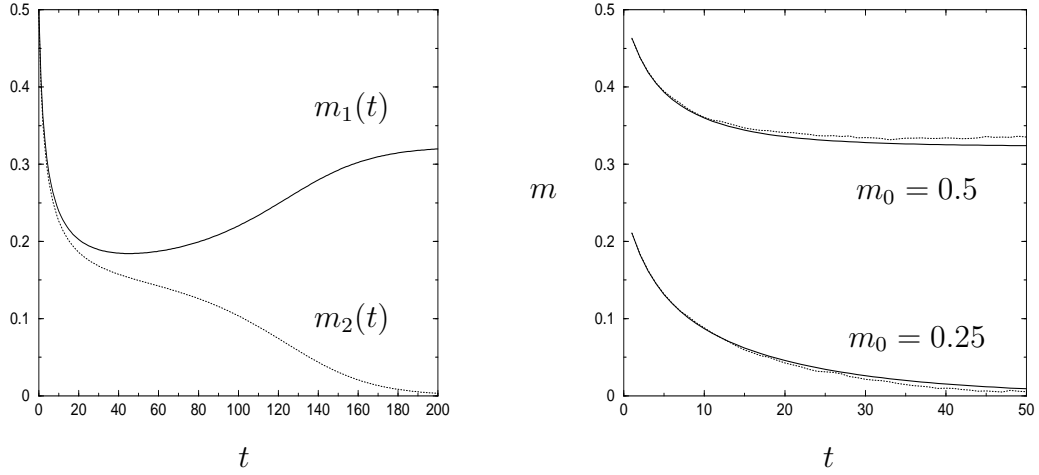
Figure 5. Left: evolution of recall overlaps m_1 (solid line) and m_2 (dashed line), as described by equation (40), following the nearly symmetrical initialization $(m_1(0), m_2(0)) = (0.50, 0.49)$ and for control parameters $\{T = 0.5, \ c = 10, \ p = 4\}$. Right: comparison between theory (i.e. the nonlinear map (39)) and numerical simulations, following the pure initial conditions $m_0 = 0.25$ (dashed: theory; dotted: simulations) and $m_0 = 0.5$ (solid: theory; short dashed: simulations). In both cases the control parameters were $\{T = 0.5, \ c = 10, \ p = 4\}$. The simulations were carried out with $N = 128,000$ and averaged over ten runs.

This recovers the corresponding equation in [30]. It is fairly straightforward to expand (39) for small $m(t)$ and show that the bifurcation corresponding to (38) has $m \neq 0$, which confirms that (38) indeed marks a P→R transition, as claimed. Iteration of (39) until stationarity allows us to find the stationary overlaps $m(\infty)$ for any given value of the control parameters. Examples are plotted in figure 4, both as functions of T (left) and as functions of α (right). The locations of the critical points, where $m(\infty)$ vanishes, are seen to be fully consistent with the phase diagram of figure 3, as they should.

Let us finally make a mixed state ansatz where the system has a non-vanishing overlap with two patterns, i.e. $m_{\boldsymbol{\xi}}(t) = \xi^1 m_1(t) + \xi^2 m_2(t)$ (such that $m_1(t) = \langle \xi^1 m_{\boldsymbol{\xi}}(t) \rangle_{\boldsymbol{\xi}}$ and $m_2(t) = \langle \xi^2 m_{\boldsymbol{\xi}}(t) \rangle_{\boldsymbol{\xi}}$). Again this ansatz gives self-consistent solutions of (35), with for $\theta(t) = 0$ the two recall overlaps $\{m_1, m_2\}$ now evolving according to

$$
\begin{pmatrix} m_1(t+1) \\ m_2(t+1) \end{pmatrix} = \frac{1}{2} \sum_{k \geq 0} \frac{e^{-c} c^k}{k!} \left\langle \dots \left\langle \tanh(\frac{\beta}{c} [\sum_{0 < \ell \leq k} \xi_\ell^1 + \sum_{0 < \ell \leq k} \xi_\ell^2 + \sum_{\mu > 2} \sum_{0 < \ell \leq k} \xi_\ell^\mu]) \right. \right.
$$
$$
\times \left. \left. \begin{pmatrix} \prod_{0 < \ell \leq k}[1 + \xi_\ell^1 m_1(t) + \xi_\ell^2 m_2(t)] + \prod_{0 < \ell \leq k}[1 + \xi_\ell^1 m_1(t) - \xi_\ell^2 m_2(t)] \\ \prod_{0 < \ell \leq k}[1 + \xi_\ell^1 m_1(t) + \xi_\ell^2 m_2(t)] + \prod_{0 < \ell \leq k}[1 - \xi_\ell^1 m_1(t) + \xi_\ell^2 m_2(t)] \end{pmatrix} \right\rangle_{\boldsymbol{\xi}_1} \dots \right\rangle_{\boldsymbol{\xi}_k} \quad (40)
$$

This can also be written in combinatorial form, by counting the various occurrences of specific values for (ξ_ℓ^1, ξ_ℓ^2) among the k pairs, as well as the statistics of the various summations over pattern components. Equation (40) can be used, for instance, to demonstrate the instability of 2-mixtures (known from fully connected models) in favour of pure states; see e.g. figure 5 (left panel). In the same figure (right panel) we

also compare the overlap evolution as predicted by (39) to the result of carrying out numerical simulations, with $N = 128,000$ spins, and with different initial conditions. The agreement, although not perfect, is quite satisfactory.

5. Arbitrary connectivity symmetry

Equation (17) is closed and exact, for arbitrary degrees of symmetry, and arbitrary choices of the bond distribution $\tilde{P}(J)$. For $\epsilon > 0$, where the connectivity is no longer strictly asymmetric, it is no longer possible to simplify (17) in a manner similar to what was possible for $\epsilon = 0$. It closes only in the space defined by the conditional path probabilities $P(\boldsymbol{\sigma}|\boldsymbol{\theta})$. For continuous bonds one will have continuous fields $\boldsymbol{\theta}$, so even on finite time-scales the order parameter space is already infinite dimensional. For discrete bonds, e.g. $\pm J$ random ones, the required fields $\boldsymbol{\theta}$ are also discrete, and hence the space is finite dimensional (although the dimension increases exponentially with time). Careful inspection of the causality structure of (17) shows that if the largest time argument in the paths $\boldsymbol{\sigma}_\ell$ is t, then the distributions $P(\boldsymbol{\sigma}_\ell|J_\ell\boldsymbol{\sigma}/c)$ in the right-hand side of (17) only depend on those entries of the path vector $\boldsymbol{\sigma}$ with time label $t-2$ at most. Hence every spin variable couples to the local field generated by itself at times up to 2 steps previously or earlier, which is indeed the time needed for the effect of a spin change to propagate along a bond (or multiple bonds) and return.

5.1. Numerical solution for short times

For short times $t \leq t_{\max}$ it is perfectly straightforward and simple to solve the macroscopic laws (17) numerically, by iteration. Especially if we restrict ourselves to bond distributions of the form $\tilde{P}(J') = \frac{1}{2}(1 + \eta)\delta(J' - J) + \frac{1}{2}(1 - \eta)\delta(J' + J)$, our equations close in a finite-dimensional space. Upon defining the new order parameters $W(\boldsymbol{\sigma}|\boldsymbol{\sigma}') = P(\boldsymbol{\sigma}|\frac{J\boldsymbol{\sigma}'}{c})$, with $\boldsymbol{\sigma}' \in \{-1, 1\}^{t_{\max}} \bigcup \{\mathbf{0}\}$, and writing $J_\ell = J\tau_\ell$ we find closure in terms of

$$W(\boldsymbol{\sigma}|\boldsymbol{\sigma}') = \sum_{k \geq 0} \frac{e^{-c}c^k}{k!} \prod_{0 < \ell \leq k} \left\{ \sum_{\tau_\ell = \pm 1} \frac{1}{2}(1 + \eta\tau_\ell) \sum_{\boldsymbol{\sigma}_\ell} [\epsilon W(\boldsymbol{\sigma}_\ell|\tau_\ell\boldsymbol{\sigma}) + (1 - \epsilon)W(\boldsymbol{\sigma}_\ell|\mathbf{0})] \right\}$$
$$\times p(\sigma(0)) \prod_{t \geq 0} \frac{e^{\beta\sigma(t+1)\{\theta(t) + \frac{J}{c}[\sigma'(t) + \sum_{0 < \ell \leq k} \tau_\ell\sigma_\ell(t)]\}}}{2\cosh(\beta\{\theta(t) + \frac{J}{c}[\sigma'(t) + \sum_{0 < \ell \leq k} \tau_\ell\sigma_\ell(t)]\})} \tag{41}$$

Clearly, for $\epsilon = 0$ (strict asymmetry) we return to (18). Examples of the result of iterating (41) numerically for $\boldsymbol{\theta} = \mathbf{0}$ (no external fields, only the internal ones $\boldsymbol{\theta}'$) and subsequently calculating the magnetizations $m(t) = \sum_{\boldsymbol{\sigma}} \sigma(t)W(\boldsymbol{\sigma}|\mathbf{0})$, are shown in figure 6. These magnetization values are tested against the corresponding measurements in numerical simulations, with system size $N = 64,000$ and averaged over 20 runs. Here $\eta \in \{\frac{2}{5}, \frac{4}{5}\}$ with in both cases $c = 2$, $\epsilon = 1$ and $\beta J = 3$. We observe excellent agreement between theory and experiment, confirming the correctness of our basic result (17) also away from strict asymmetry. We notice in addition the familiar macroscopic oscillations
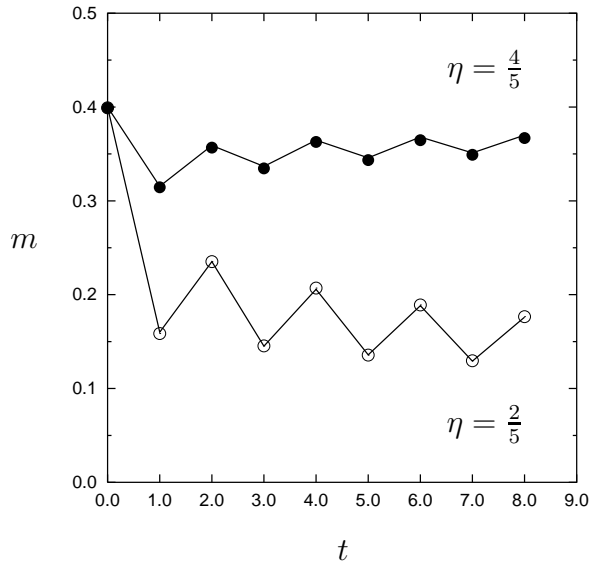
Figure 6. Evolution of the magnetization in the $\pm J$ spin-glass on a symmetric ($\epsilon = 1$) random finitely connected Poissonian graph, without external fields. We compare the predictions of the theory (points connected by line segments), to that observed in numerical simulations (markers), for short times and following an initial state with $m_0 = 2/5$. Top curve and full circles: $\eta = 4/5$. Lower curve and open circles: $\eta = 2/5$. The simulations were carried out with $N = 64,000$, and all measurements were averaged over 20 runs. In both scenarios $c = 2$ and $\beta J = 3$.

which one tends to have in parallel dynamics spin systems with (partly) negative bonds. As expected the magnitude of these oscillations reduces with increasing values of η (where the fraction of positive bonds increases); repeating these experiments for $\eta = 1$ (positive bonds only) would show oscillations to be absent. In view of the exponential growth of the number of dynamical order parameters with time, it is not feasible in practice to iterate beyond times of the order of magnitude shown in the figure.

5.2. Numerical solution of the stationary state

Detailed balance holds only for $\epsilon = 1$, hence only then will one be able to use equilibrium statistical mechanical techniques for analyzing the stationary state. Due to the synchronous updating of the spins (1), the $\epsilon = 1$ equilibrium state is not of a Boltzmann form, but involves Peretto's pseudo-Hamiltonian [33] (which depends on the noise level T). Away from $\epsilon = 1$ the only way to obtain information on the stationary state is to concentrate on the stationary solution(s) of our dynamical theory (17).

The difficulty in doing this numerically, when $\epsilon > 0$, lies in the need to take into account the entire history. Hence in practice one is forced to truncate the extent to which history is taken into account explicitly at some appropriate memory depth λ, and average over those spin values assumed to be too remote to have a non-negligible effect in the right-hand side of (17). The resulting truncated equations are iterated until the
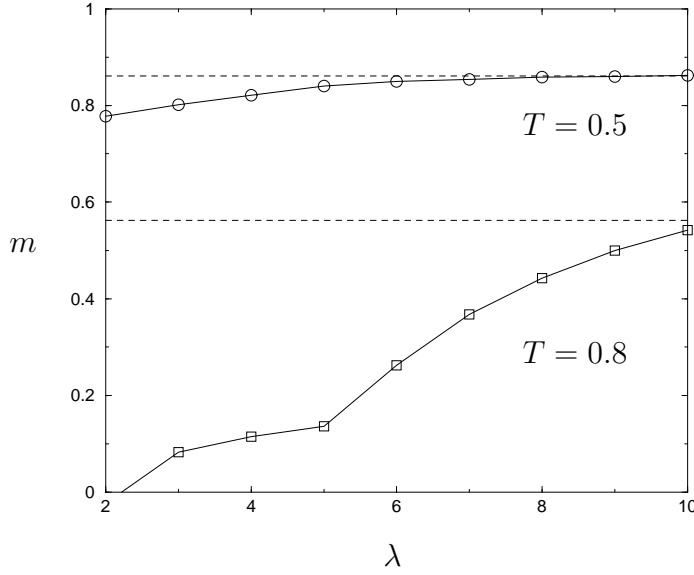
Figure 7. Stationary state magnetizations in the $\pm J$ spin-glass on a symmetric ($\epsilon = 1$) random finitely connected Poissonian graph, without external fields. We compare the predictions of the present dynamical theory with truncated paths (connected markers), to the values obtained from finite connectivity equilibrium replica theory based on Peretto's pseudo-Hamiltonian and within the RS ansatz (dashed horizontal lines), as a function of the memory depth λ of the single spin paths. Data are shown for $T = 0.5$ (upper, circles), and for $T = 0.8$ (lower, squares). In both cases $c = 5$.

magnetization has become stationary. To speed up the equilibration process we used a stochastic interpretation of (17), in the spirit of population dynamics algorithms: at each iteration step a number k was drawn from a Poissonian distribution, upon which k bond strenghts J_ℓ were selected randomly from the bond distribution $\tilde{P}(J)$, and k λ-step spin trajectories $\boldsymbol{\sigma}_\ell$ were drawn (given that truncation was carried out at λ steps into the past) from the distribution $P(\boldsymbol{\sigma}_\ell | J_\ell \boldsymbol{\sigma}/c)$. The new distribution $P(\boldsymbol{\sigma} | \boldsymbol{\theta}')$ was then calculated according to

$$P_{\text{new}}(\boldsymbol{\sigma} | \boldsymbol{\theta}') = P_{\text{old}}(\boldsymbol{\sigma} | \boldsymbol{\theta}') + \Delta. \prod_{t=t_m-\lambda+1}^{t_{\max}} \frac{e^{\beta\sigma(t+1)[\theta(t)+\sum_{\ell \leq k} \frac{J_\ell \sigma_\ell(t)}{c} + \theta'(t)]}}{2\cosh(\beta[\theta(t) + \sum_\ell \leq k \frac{J_\ell \sigma_\ell(t)}{c} + \theta'(t)])} \quad (42)$$

where Δ is a small positive number. We subsequently normalized the new distribution $P_{\text{new}}(\boldsymbol{\sigma} | \boldsymbol{\theta}')$, and moved to the next iteration step. In figure 7 we present some results of the above numerical procedure for a fully symmetrically diluted ferromagnet, i.e. $\epsilon = 1$, with $c = 5$ and for two different temperature values $T = 0.5$ and $T = 0.8$. We truncated the spin paths after up to $\lambda = 10$ past iteration steps. The reason for choosing $\epsilon = 1$, i.e. the detailed balance limit, is that it allows for a convenient comparison with predictions obtained within equilibrium theory (the finite connectivity ensemble analysis based on the Peretto pseudo-Hamiltonian, following [15]). In the latter theory one can obtain explicit independent predictions for the equilibrium magnetization, at least within the RS ansatz and upon solving for the various effective field distributions using standard

population dynamics algorithms. The result is figure 7, which gives an indication of the extent to which memory is to be taken into account (17), which is seen to increase as one approaches the critical temperature. It also confirms the correctness of our theory in the stationary state, complementing the short-time validation of figure 6.

5.3. Structural properties and approximate stationary solution at $\epsilon = 1$

Finally we show how one might go beyond numerical analysis of our equations, and obtain both a better understanding of the structural properties of (17) as well as explicit approximate stationary state solutions. For simplicity we send initial and final times to minus and plus infinity, respectively, we choose zero external fields, and we investigate the following ansatz for a stationary state, in terms of an effective field distribution:

$$P(\boldsymbol{\sigma}|\boldsymbol{\theta}) = \int \mathrm{d}h \; W(h) \prod_t \frac{e^{\beta\sigma(t+1)[h+\theta(t)]}}{2\cosh(\beta[h+\theta(t)])} \tag{43}$$

To compactify our notation we will abbreviate $\prod_t[\frac{1}{2}\sum_{\sigma(t)=\pm 1}]f(\boldsymbol{\sigma}) = \langle f(\boldsymbol{\sigma})\rangle_{\boldsymbol{\sigma}}$. We insert the ansatz (43) into the right-hand side of (17), which gives

$$\mathrm{RHS} = \sum_{k\geq 0} \frac{e^{-c}c^k}{k!} \left\langle \prod_{0<\ell\leq k} \left\{ \int \mathrm{d}h_\ell \mathrm{d}J_\ell \tilde{P}(J_\ell) W(h_\ell) \prod_t \frac{e^{\beta\sigma_\ell(t+1)[h_\ell+\frac{J_\ell\sigma(t)}{c}]}}{\cosh(\beta[h_\ell+\frac{J_\ell\sigma(t)}{c}])} \right\} \right.$$

$$\left. \times \prod_t \frac{e^{\beta\sigma(t+1)[\theta(t)+\sum_{0<\ell\leq k}\frac{J_\ell\sigma_\ell(t)}{c}]}}{2\cosh(\beta[\theta(t)+\sum_{0<\ell\leq k}\frac{J_\ell\sigma_\ell(t)}{c}])} \right\rangle_{\boldsymbol{\sigma}_1...\boldsymbol{\sigma}_k} \tag{44}$$

Since all complications of the $\epsilon > 0$ dynamics stem from the dependence of $P(\boldsymbol{\sigma}_\ell|\frac{J_\ell}{c}\boldsymbol{\sigma})$ on $\boldsymbol{\sigma}$, we next try to concentrate all $\{\sigma(t)\}$ in exponentials using the simple identity

$$\cosh[\beta(a+b\sigma)] = A(a,b)e^{\beta B(a,b)\sigma}, \qquad \begin{array}{l} A(a,b) = \sqrt{\cosh(\beta[a{+}b])\cosh(\beta[a{-}b])} \\ B(a,b) = \frac{1}{2\beta}\log\left[\frac{\cosh(\beta[a{+}b])}{\cosh(\beta[a{-}b])}\right] \end{array} \tag{45}$$

This allows us to write (44) in the form

$$\mathrm{RHS} = \sum_{k\geq 0} \frac{e^{-c}c^k}{k!} \prod_{0<\ell\leq k} \left\{ \int \mathrm{d}h_\ell \mathrm{d}J_\ell \tilde{P}(J_\ell) W(h_\ell) \right\} \prod_t \frac{e^{\beta\sigma(t+1)[\theta(t)-\sum_{\ell\leq k}B(h_\ell,\frac{J_\ell}{c})]}}{\prod_{\ell\leq k}A(h_\ell,\frac{J_\ell}{c})}$$

$$\times \prod_t \left\langle \frac{e^{\beta\sum_{\ell\leq k}\sigma_\ell[h_\ell+\frac{J_\ell}{c}[\sigma(t-1)+\sigma(t+1)]]}}{2\cosh(\beta[\theta(t)+\sum_{0<\ell\leq k}\frac{J_\ell\sigma_\ell}{c}])} \right\rangle_{\sigma_1...\sigma_k} \tag{46}$$

We note that $\frac{1}{2}[\sigma(t-1)+\sigma(t+1)] \in \{-1,0,1\}$. In order to transport also the $\{\sigma(t)\}$ occurrences in the last line to exponentials, we use the following identity:

$$S \in \{-1,0,1\}: \quad f(S) = Ce^{\beta DS + \beta FS^2}, \qquad \begin{array}{l} C = f(0) \\ D = \frac{1}{2\beta}\log\left[\frac{f(1)}{f(-1)}\right] \\ F = \frac{1}{2\beta}\log\left[\frac{f(1)f(-1)}{f^2(0)}\right] \end{array} \tag{47}$$

Application to our present problem gives

$$\mathrm{RHS} = \sum_{k\geq 0} \frac{e^{-c}c^k}{k!} \prod_{0<\ell\leq k} \left\{ \int \mathrm{d}h_\ell \mathrm{d}J_\ell \tilde{P}(J_\ell) W(h_\ell) \right\} \prod_t \left[\frac{C_{k,t}[\{h,J\}]e^{\frac{1}{2}\beta F_{k,t}[\{h,J\}]}}{\prod_{\ell\leq k}A(h_\ell,\frac{J_\ell}{c})} \right]$$

$$\times \prod_t e^{\beta\sigma(t+1)\left[\theta(t)-\sum_{\ell\leq k}B(h_\ell,\frac{J_\ell}{c})+\frac{1}{2}D_{k,t}[\{h,J\}]+\frac{1}{2}D_{k,t+2}[\{h,J\}]+\frac{1}{2}F_{k,t}[\{h,J\}]\sigma(t-1)\right]} \quad (48)$$

with the form factors

$$C_{k,t}[\{h,J\}] = \left\langle \frac{e^{\beta\sum_{\ell\leq k}\sigma_\ell h_\ell}}{2\cosh(\beta[\theta(t)+\sum_{0<\ell\leq k}\frac{J_\ell\sigma_\ell}{c}])} \right\rangle_{\sigma_1...\sigma_k} \quad (49)$$

$$D_{k,t}[\{h,J\}] = \frac{1}{2\beta}\log\left[\frac{\left\langle\frac{e^{\beta\sum_{\ell\leq k}\sigma_\ell[h_\ell+\frac{2J_\ell}{c}]}}{2\cosh(\beta[\theta(t)+\sum_{0<\ell\leq k}\frac{J_\ell\sigma_\ell}{c}])}\right\rangle_{\sigma_1...\sigma_k}}{\left\langle\frac{e^{\beta\sum_{\ell\leq k}\sigma_\ell[h_\ell-\frac{2J_\ell}{c}]}}{2\cosh(\beta[\theta(t)+\sum_{0<\ell\leq k}\frac{J_\ell\sigma_\ell}{c}])}\right\rangle_{\sigma_1...\sigma_k}}\right] \quad (50)$$

$$F_{k,t}[\{h,J\}] = \frac{1}{2\beta}\log\left[\frac{\left\langle\frac{e^{\beta\sum_{\ell\leq k}\sigma_\ell[h_\ell+\frac{2J_\ell}{c}]}}{2\cosh(\beta[\theta(t)+\sum_{0<\ell\leq k}\frac{J_\ell\sigma_\ell}{c}])}\right\rangle_{\sigma_1...\sigma_k}\left\langle\frac{e^{\beta\sum_{\ell\leq k}\sigma_\ell[h_\ell-\frac{2J_\ell}{c}]}}{2\cosh(\beta[\theta(t)+\sum_{0<\ell\leq k}\frac{J_\ell\sigma_\ell}{c}])}\right\rangle_{\sigma_1...\sigma_k}}{\left\langle\frac{e^{\beta\sum_{\ell\leq k}\sigma_\ell h_\ell}}{2\cosh(\beta[\theta(t)+\sum_{0<\ell\leq k}\frac{J_\ell\sigma_\ell}{c}])}\right\rangle_{\sigma_1...\sigma_k}^2}\right] \quad (51)$$

Expression (48) is still fully exact, but involves potentially time-dependent form factors and a retarded self-interaction. We now use (48) for constructing an approximate stationary solution of equation (17) for large c. In Appendix B we derive

$$D_{k,t}[\{h,J\}] = \frac{2}{c}\sum_{\ell\leq k}J_\ell\tanh[\beta h_\ell] + \mathcal{O}(\frac{1}{c}) \qquad F_{k,t}[\{h,J\}] = \mathcal{O}(\frac{1}{c}) \quad (52)$$

(obviously, alternative choices for the scaling with c of the bonds would lead to different expressions). Causality would have been violated in (48) as soon as $D_t[\{h,J\}]$ were to depend on t; it is thus satisfactory to see in (52) that $\theta(t)$ indeed drops out (the next order c^{-1} of $D_t[\{h,J\}]$ is again found to be independent of t). In combination, if we also use explicit normalization, this results in the following approximated solution of (17):

$$P(\boldsymbol{\sigma}|\boldsymbol{\theta}) = \int dh\, W(h)\prod_t \frac{e^{\beta\sigma(t+1)[\theta(t)+h]}}{2\cosh(\beta[\theta(t)+h])} \quad (53)$$

$$W(h) = \sum_{k\geq 0}\frac{e^{-c}c^k}{k!}\prod_{0<\ell\leq k}\left\{\int dh_\ell dJ_\ell \tilde{P}(J_\ell)W(h_\ell)\right\}$$

$$\times \delta\left[h-\frac{2}{c}\sum_{\ell\leq k}J_\ell\tanh[\beta h_\ell] + \frac{1}{2\beta}\sum_{\ell\leq k}\log\left[\frac{\cosh(\beta[h_\ell+\frac{J_\ell}{c}])}{\cosh(\beta[h_\ell-\frac{J_\ell}{c}])}\right] + \mathcal{O}(\frac{1}{c})\right] \quad (54)$$

The last equation (54) can be rewritten as

$$W(h) = \sum_{k\geq 0}\frac{e^{-c}c^k}{k!}\prod_{0<\ell\leq k}\left\{\int dh_\ell dJ_\ell \tilde{P}(J_\ell)W(h_\ell)\right\}$$

$$\times \delta\left[h-\frac{1}{\beta}\sum_{\ell=1}^k \text{arctanh}[\tanh(\frac{\beta J_\ell}{c})\tanh(\beta h_\ell)] + \mathcal{O}(\frac{1}{c})\right] \quad (55)$$

In leading order in c^{-1} this is identical to the replica symmetric equilibrium solution of the sequential dynamics version of our model, as derived in [3] (on the basis of [15] one expects the RS equilibrium solutions of sequential and parallel dynamics to be identical).

Solutions of the simple form (43) or similar, if they exist, are expected to be typical of parallel as opposed to sequential dynamics. We realize that the above analysis as yet falls short of leading to exact solutions of our macroscopic equations, but it does suggest possibilities for deriving approximate solutions in a controlled manner. The latter could then also possibly be employed for $\epsilon < 1$, where equilibrium analysis is not an option.

6. Discussion

In this paper we used the generating functional analysis methods of De Dominicis to analyze the dynamics of finitely connected Ising spin models with parallel dynamics, random bonds, and controlled degrees of connectivity symmetry. We have derived an exact equation, valid in the infinite system size limit, for the dynamic order parameter of our problem. This order parameter represents the probability for finding a single-site path in configuration space, given a (finite) deviation in the local external field at that site. It generalizes the dynamic order parameters usually found for disordered systems with full or with diverging random connectivity, viz. correlation- and response functions.

We have applied our dynamical theory first to models with strictly asymmetric connectivity. Here there is no effective retarded self-interaction in the problem, and our theory consequently simplifies (for instance, one never finds spin-glass states). Applications of the resulting dynamical equations include finitely connected random bond models (exhibiting continuous ferromagnetic phase transitions), and finitely connected recurrent neural network models (exhibiting recall transitions). Numerical simulations support our findings and predictions. Next we turned to models with (partly) symmetric connectivity, where the order parameter equations are much more complicated. We first showed how our equations can be solved iteratively for the first few time-steps (although the computation required grows exponentially with time, which limits what can be done in practice), and how the resulting predictions find perfect confirmation in numerical simulations. The stationary state solution of our dynamical theory was approximated both numerically (by truncating the effective memory of the non-Markovian macroscopic equations) and analytically (upon making a simple ansatz in the language of effective field distributions). In the latter case we had to resort to an approximation, which is correct in leading non-trivial order in c^{-1}, and which up to that order reproduces the self-consistent equation which was found earlier for the equilibrium effective field distribution in RS approximation.

We now have an exact dynamical theory for finitely connected random bond Ising spin models, albeit in the form of equations which are generally hard to solve (which, given past experience with statics and dynamics of disordered systems, will not come as a surprise). In this paper we also hope to have shown that solution, under certain conditions and/or in special limits, is nevertheless not ruled out either. Moreover, the availability of an exact macroscopic theory is vital for the systematic development of practical approximations, and also to serve as a yardstick against which to test alternative (and perhaps simpler) dynamical theories with the ambition of exactness.

Acknowledgment

References

[1] Viana L and Bray A J 1985 *J. Phys. C* **18** 3037
[2] Kanter I and Sompolinsky H 1987 *Phys. Rev. Lett.* **58** 164
[3] Mezard M and Parisi G 1987 *Europhys. Lett.* **3** 1067
[4] Mottishaw P and De Dominicis C 1987 *J. Phys. A* **20** L375
[5] Wong K Y and Sherrington D 1988 *J. Phys. A* **21** L459
[6] Monasson R 1998 *J. Phys. A* **31** 513
[7] Murayama T, Kabashima Y, Saad D and Vicente R 2000 *Phys. Rev. E* **62** 1577
[8] Nakamura K, Kabashima Y and Saad D 2001 *Europhys. Lett.* **56** 610
[9] Nishimori H 2001 *Statistical Physics of Spin Glasses and Information Processing* (Oxford: University Press)
[10] Kirkpatrick S and Selman B 1994 *Science* **264** 1297
[11] Monasson R and Zecchina R 1998 *Phys. Rev. E* **56** 1357
[12] Monasson R and Zecchina R 1998 *J. Phys. A* **31** 9209
[13] Monasson R, Zecchina R, Kirkpatrick S, Selman B and Troyansky L 1999 *Nature* **400** 133
[14] Wemmenhove B and Coolen A C C 2003 *J. Phys. A* **36** 9617
[15] Perez Castillo I and Skantzos N S 2003 *preprint* cond-mat/0309655
[16] Gitterman A 2000 *J. Phys. A: Math. Gen* **33** 8373
[17] Nikoletopoulos T, Coolen A C C, Pérez Castillo I, Skantzos N S, Hatchett J P L and Wemmenhove B 2004 *preprint* cond-mat/0402504
[18] Mezard M, Parisi G and Virasoro M A 1987 *Spin Glass Theory and Beyond* (Singapore: World Scientific)
[19] de Dominicis C and Goldschmidt Y Y 1989 *J. Phys. A* **22** L775
[20] Lai P Y and Goldschmidt Y Y 1990 *J. Phys. A* **23** 3329
[21] Goldschmidt Y Y and de Dominicis C 1990 *Phys. Rev. B* **41** 2184
[22] Parisi G and Tria F 2002 *preprint* cond-mat/0207144
[23] Semerjian G and Weigt M 2004 *preprint* cond-mat/0402451
[24] Semerjian G and Cugliandolo L F 2003 *Europhys. Lett.* **61** 247
[25] De Dominicis C, 1978, *Phys. Rev. B* **18** 4913
[26] Crisanti A and Sompolinsky H 1987 *Phys. Rev. A* **36** 4922
[27] Crisanti A and Sompolinsky H 1988 *Phys. Rev. A* **37** 4865
[28] Rieger H, Schreckenberg M and Zittartz J 1989 *Z. Phys. B* **74** 527
[29] Düring A, Coolen A C C and Sherrington D 1998 *J. Phys. A: Math. Gen.* **31** 8607
[30] Derrida B, Gardner E and Zippelius A 1987 *Europhys. Lett.* **4** 167
[31] Kree R and Zippelius A 1991 in *Models of Neural Networks I* Domany R, van Hemmen JL and Schulten K (Eds) (Berlin: Springer) 193
[32] van Hemmen J L 1987 *Phys. Rev. A* **36** 1959
[33] Peretto P 1984 *Biol. Cybern.* **50** 51

Appendix A. Absence of spin-glass phase for asymmetric connectivity

Here we show analytically that for asymmetric connectivity, i.e. $\epsilon = 0$, there cannot be a spin-glass phase. The spin-glass order parameter $q \in [0, 1]$ is to be solved from the fixed-point equation $G(q) = q$, where

$$G(q) = \sum_{k \geq 0} \frac{e^{-c}c^k}{k!} \prod_{0 < \ell \leq k} \left\{ \frac{1}{4} \sum_{\sigma_\ell \sigma'_\ell} (1 + q\sigma_\ell\sigma'_\ell) \int dJ_\ell \, \tilde{P}(J_\ell) \right\}$$
$$\times \tanh[\frac{\beta}{c} \sum_{\ell \leq k} J_\ell\sigma_\ell] \tanh[\frac{\beta}{c} \sum_{\ell \leq k} J_\ell\sigma'_\ell] \tag{A.1}$$

We note that $G(0) = 0$, and that $G(q) \leq 1$ for all $q \in [0, 1]$. We prove the absence of non-trivial fixed-points of $G(q)$ by showing that $G''(q) > 0$ for $q > 0$, which immediately implies that $G(q) < q$ for $0 < q \leq 1$. Working out the second derivative of $G(q)$ gives

$$G''(q) = \sum_{k \geq 2} \frac{e^{-c}c^k}{(k-2)!} \prod_{0 < \ell \leq k} \left\{ \int dJ_\ell \, \tilde{P}(J_\ell) \right\} \prod_{2 < \ell \leq k} \left\{ \frac{1}{4} \sum_{\sigma_\ell \sigma'_\ell} (1 + q\sigma_\ell\sigma'_\ell) \right\}$$
$$\times \left[\frac{1}{4} \sum_{\sigma_1\sigma_2} \sigma_1\sigma_2 \tanh[\frac{\beta}{c} \sum_{\ell=1}^k J_\ell\sigma_\ell] \right] \left[\frac{1}{4} \sum_{\sigma'_1\sigma'_2} \sigma'_1\sigma'_2 \tanh[\frac{\beta}{c} \sum_{\ell=1}^k J_\ell\sigma'_\ell] \right] \tag{A.2}$$

Here we need the objects $\psi(S)$ and $\psi(S')$, where $S = \frac{\beta}{c} \sum_{\ell=3}^k J_\ell\sigma_\ell$ and $S' = \frac{\beta}{c} \sum_{\ell=3}^k J_\ell\sigma'_\ell$:

$$\psi(S) = \frac{1}{4} \sum_{\sigma_1\sigma_2} \sigma_1\sigma_2 \tanh[S + \frac{\beta}{c}(J_1\sigma_1 + J_2\sigma_2)] \tag{A.3}$$

$$= \frac{1}{4} \sum_{\sigma_1\sigma_2} \sigma_1\sigma_2 \frac{\left(\tanh[S] + \tanh[\frac{\beta}{c}(J_1\sigma_1 + J_2\sigma_2)] \right) \left(1 - \tanh[S] \tanh[\frac{\beta}{c}(J_1\sigma_1 + J_2\sigma_2)] \right)}{1 - \tanh^2[S] \tanh^2[\frac{\beta}{c}(J_1\sigma_1 + J_2\sigma_2)]}$$

$$= \frac{1}{2} \tanh[S] \left\{ \frac{1 - \tanh^2[\frac{\beta}{c}(J_1 + J_2)]}{1 - \tanh^2[S] \tanh^2[\frac{\beta}{c}(J_1 + J_2)]} - \frac{1 - \tanh^2[\frac{\beta}{c}(J_1 - J_2)]}{1 - \tanh^2[S] \tanh^2[\frac{\beta}{c}(J_1 - J_2)]} \right\}$$

$$= \frac{\tanh[S](1 - \tanh^2[S]) \left[\tanh^2[\frac{\beta}{c}(J_1 - J_2)] - \tanh^2[\frac{\beta}{c}(J_1 + J_2)] \right]}{2 \left[1 - \tanh^2[S] \tanh^2[\frac{\beta}{c}(J_1 + J_2)] \right] \left[1 - \tanh^2[S] \tanh^2[\frac{\beta}{c}(J_1 - J_2)] \right]}$$

It follows that

$$\psi(S)\psi(S') = \tanh[S] \tanh[S'] W(|S|, |S'|) \tag{A.4}$$

in which the function $W(|S|, |S'|)$ is srictly non-negative and invariant under permutation of its arguments. Since S and S' are zero-average but positively correlated random variables for $q > 0$, one concludes that $G''(q) > 0$.

Appendix B. Evaluation of form factors $D_{k,t}[\{h, J\}]$ and $F_{k,t}[\{h, J\}]$

Here we calculate the form factors (50) and (51) for large c, where we know that in the Poissonian sums the physics will be dominated by those terms with $k = \mathcal{O}(c)$. Both (50) and (51) involve averages over $\{\sigma_1, \ldots, \sigma_k\}$, with $p(\sigma_1, \ldots, \sigma_k) = 2^{-k}$, and can be

written in the following form:

$$D_{k,t}[\{h, J\}] = \frac{1}{2\beta} \log[\phi(1)/\phi(-1)] \tag{B.1}$$

$$F_{k,t}[\{h, J\}] = \frac{1}{2\beta} \{\log[\phi(1)/\phi(0)] + \log[\phi(-1)/\phi(0)]\} \tag{B.2}$$

where

$$
\begin{aligned}
\phi(u) &= \left\langle \frac{e^{\beta \sum_{\ell \leq k} \sigma_\ell h_\ell + \frac{2u\beta}{c} \sum_{\ell \leq k} \sigma_\ell J_\ell}}{2 \cosh(\beta[\theta(t) + \sum_{0 < \ell \leq k} \frac{J_\ell \sigma_\ell}{c}])} \right\rangle_{\sigma_1 \dots \sigma_k} \\
&= \int \frac{dy d\hat{y}}{2\pi} \frac{e^{i\hat{y}y + 2uy}}{2 \cosh[\beta\theta(t) + y]} \left\langle e^{\beta \sum_{\ell \leq k} \sigma_\ell [h_\ell - \frac{i\hat{y} J_\ell}{c}]} \right\rangle_{\sigma_1 \dots \sigma_k} \\
&= \int \frac{dy d\hat{y}}{2\pi} \frac{e^{i\hat{y}y + 2uy}}{2 \cosh[\beta\theta(t) + y]} \prod_{\ell \leq k} \cosh[\beta(h_\ell - \frac{i\hat{y} J_\ell}{c})] \\
&= \prod_{\ell \leq k} \cosh[\beta h_\ell] . \int \frac{dy d\hat{y}}{2\pi} \frac{e^{i\hat{y}y + 2uy}}{2 \cosh[\beta\theta(t) + y]} e^{-\frac{i\beta\hat{y}}{c} \sum_{\ell \leq k} J_\ell \tanh[\beta h_\ell] + \mathcal{O}(\frac{1}{c})} \\
&= \prod_{\ell \leq k} \cosh[\beta h_\ell] . \frac{e^{\frac{2\beta u}{c} \sum_{\ell \leq k} J_\ell \tanh[\beta h_\ell] + \mathcal{O}(\frac{1}{c})}}{2 \cosh[\beta(\theta(t) + \frac{1}{c} \sum_{\ell \leq k} J_\ell \tanh[\beta h_\ell])]}
\end{aligned}
\tag{B.3}
$$

Hence

$$D_{k,t}[\{h, J\}] = \frac{2}{c} \sum_{\ell \leq k} J_\ell \tanh[\beta h_\ell] + \mathcal{O}(\frac{1}{c}) \tag{B.4}$$

$$F_{k,t}[\{h, J\}] = \mathcal{O}(\frac{1}{c}) \tag{B.5}$$

Working out higher orders in c^{-1} is in principle straightforward. Including $\mathcal{O}(c^{-1})$ would convert the result of the $\hat{y}$ integration in our representation of the function $\phi(u)$ from a δ-distribution for y into a Gaussian integral, which can in turn be done analytically.